

Surface strengthening of AISI4140 by cavitation peening

Alexander Klumpp^{a,*}, Franziska Lienert^a, Stefan Dietrich^a, Hitoshi Soyama^b, Volker Schulze^a

^{a,*} Karlsruhe Institute of Technology, Germany, alexander.klumpp@kit.edu

^b Tohoku University, Japan, soyama@mm.mech.tohoku.ac.jp

Keywords: Cavitation Peening, Surface Modification, Residual Stresses, Fatigue Life

Introduction

Cavitation produces severe erosion in hydraulic machineries such as pumps and screw propellers, since severe impacts are generated when cavitation bubbles collapse. However, cavitation impacts can also be utilized to enhance materials properties in a similar way as shot peening. "Cavitation shotless peening", or simply "cavitation peening" [1], is a recently developed mechanical surface treatment which makes use of such cavitation impacts instead of conventional shot impacts. The advantages of cavitation peening (CP) are as follows: Compared to conventional shot peening, the peened surfaces are smoother after CP. This is due to the absence of shots. Furthermore, the pump pressure is lower than that of water jet peening, as cavitation impacts are used. Moreover, regions difficult to reach such as narrow tubes or tooth roots of gears can be hit by cavitation impacts.

During CP, cavitation is generated by injecting high speed water jets into water filled chambers. This type of submerged water jets with cavitation is called "cavitating jet", or a "cavitating jet in water" [2]. Soyama [3, 4] realized a cavitating jet in air without a water filled chamber, by injecting a high speed water jet into a low speed water jet which was injected into air using a concentric nozzle. In this case, it was reported that cavitation peening introduced compressive residual stresses capable of relieving micro strains, which is further described in [5]. Regarding previous report [6], the introduction of compressive residual stress by cavitating jets in air corresponds to shot peening using small shots at high velocity, whereas the introduction of residual stresses by cavitating jets in water corresponds to shot peening using large shots at low velocity. When the cavitating jet is injected in the water, secondary air bubbles follow the collapse of cavitation bubbles [7]. These secondary bubbles cause a "cushion" effect, reducing the cavitation impact energy. When the pressurized chamber is used for cavitating jets in water, the "cushion" effect is reduced by shrinking the secondary bubbles. Namely, the cavitation impact energy can be increased by using pressurized chambers.

In the present paper, three types of cavitating jets were used for cavitation peening; a cavitating jet in water with an open chamber, a cavitating jet in water with a pressurized chamber and a cavitating jet in air.

Objectives

The present study focuses on surface states after CP treatment on quenched and tempered low alloy steel AISI4140. Surface topography, residual stresses and full width at half maximum values are evaluated for each of the three different types of CP and subsequently compared to each other. By this means, the effect of CP on AISI4140 is investigated. It shall be checked whether compressive residual stresses do relieve micro strains on AISI4140 and thus affect full width at half maximum (FWHM) values. Such an effect was found after CP in air on forging die tool steel [5]. Furthermore, the influence of cavitation peening on the fatigue behavior of AISI4140 is investigated.

Moreover, this paper has another scope: Surface states after various mechanical surface treatments on AISI4140 have been investigated at Karlsruhe Institute of Technology (KIT) during the last decades. A comprehensive overview of the effects of different mechanical surface treatments on surface states of AISI4140 was given in the ICSP12 keynote [8]. Namely, these treatments are shot peening, stress peening, warm peening, micro peening, deep rolling, diamond finishing, piezo peening, laser shock treatment and high pressure water peening. By establishing a link to the latter, the effects of CP are subsequently discussed within a comparative study.

Methodology

Fig. 1 illustrates the three aforementioned types of the cavitating jet apparatus; (a) cavitating jet in water using an open chamber, (b) cavitating jet in water using a pressurized chamber and (c) cavitating jet in air. Table 1 shows the cavitating conditions for the three cases. In the case of the cavitating jet in water with the open chamber (Fig. 1 (a)), the high speed water jet was injected into the water filled open chamber [9]. In the case of Fig. 1 (b), the cavitating jet was injected into the water filled pressurized chamber [10]. In the case of cavitating jet in air, the high speed water jet was injected into the low speed water jet which was injected in air as shown in Fig. 1 (c) [4].

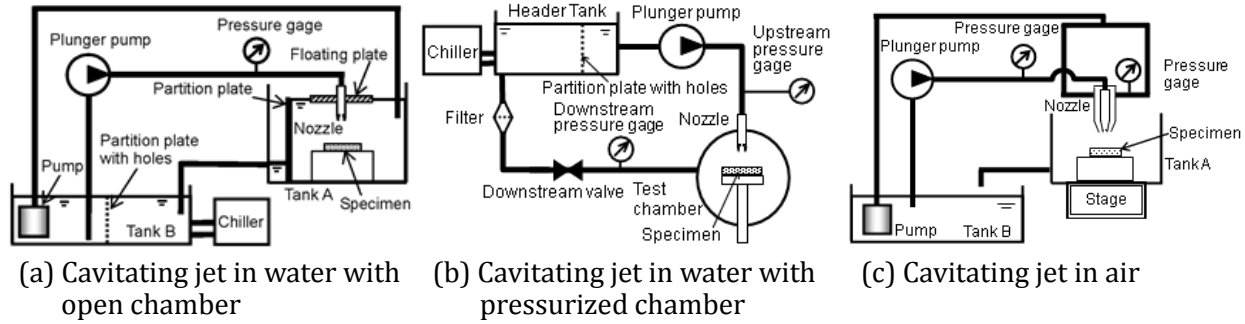


Fig. 1: Schematic diagram of cavitating jet apparatuses

The standoff distances for each case were optimized by measuring arc height or erosion rate. The arc height of type "A" Almen strip was measured at three cases changing with processing time per unit length [11], then the processing time per unit length was chosen as shown in Table 1. CP treatments were carried out at Tohoku University.

Table 1: Cavitating jet conditions

	Cavitating jet in water with open chamber	Cavitating jet in water with pressurized chamber	Cavitating jet in air
Nozzle diameter of high speed water jet d_H	2 mm	2 mm	1 mm
Nozzle diameter of low speed water jet d_L	–	–	30 mm
Standoff distance s	262 mm	80 mm	56 mm
Injection pressure of high speed water jet p_1	30 MPa	30 MPa	30 MPa
Injection pressure of low speed water jet OR Downstream pressure of nozzle p_2	– 0.1 MPa	– 0.42 MPa	0.05 MPa –
Cavitation number $\sigma \approx p_2 / p_1$	0.0033	0.0140	0.0050
Processing time per unit length t_p	6 s/mm	1.2 s/mm	20 s/mm
Arc height h_A	0.2 mm	0.2 mm	0.1 mm

Low alloy steel AISI4140 with hardness of 430 HV1 was used throughout the investigations. It was austenitized at 850 °C for 20 minutes, oil-quenched and then tempered at 450 °C for 120 minutes. Then, it was furnace-cooled to room temperature. The chemical composition is shown in Table 2.

Table 2: Chemical composition of AISI4140

Chemical composition (wt.-%)						
Fe	C	Cr	Mo	Mn	Si	Ni
Base	0.425	1.011	0.222	0.803	0.252	0.101

Flat, cuboid specimens with the dimensions 79*11*4 mm³ were used for the investigations. They were ground prior to CP treatment. Near-surface residual stresses were evaluated in the center of the 79*11 mm² surface. Cr-K_α radiation was applied on a ψ -diffractometer to evaluate the {211}- α -ferrite diffraction line at $2\theta = 156.4^\circ$. 13 ψ -tilts between -60° and $+60^\circ$ were used. Stress analysis was carried out according to the $\sin^2(\psi)$ method [12], using $E_{\{211\}} = 220$ GPa and $\nu_{\{211\}} = 0.28$ as Young's modulus and Poisson's ratio, respectively. Residual stress depth profiles were determined by incremental electrolytic layer removal. FWHM values were evaluated by averaging the values obtained from five ψ -tilts between -30° and $+30^\circ$ to avoid instrumental peak broadening. Surface roughness was evaluated using a confocal microscope of type Nanofocus μ surf. A Gaussian-type cut-off filter with a wavelength of 0.8 μ m was used for roughness evaluation. Surface layer states were characterized at Karlsruhe Institute of Technology.

Furthermore, rotating bending fatigue tests were carried out on smooth, cylindrical specimens with a gauge length of 17 mm and a thickness of 7 mm. Untreated specimens as well as specimens treated by CP in water with pressurized chamber were used. To achieve comparability with flat specimens used for residual stress evaluation, the cylindrical specimens were rotated during the peening process and the processing time per unit length was adjusted to 10 s/mm. A SincoTec test bench with a LabView-based momentum controller was used for the fatigue tests. Based on preliminary experiments, three load amplitudes in the HCF and LCF range were selected to characterize the strengthening effect of the cavitation peening treatment on AISI4140. They were chosen to be 28.6 Nm, 25.6 Nm and 23.6 Nm, leading to fictitious stresses in the extreme fiber of 850 MPa, 760 MPa and 700 MPa, respectively.

Results and analysis

Fig. 2 shows residual stresses (left) and FWHM distributions (right) for the three types of CP.

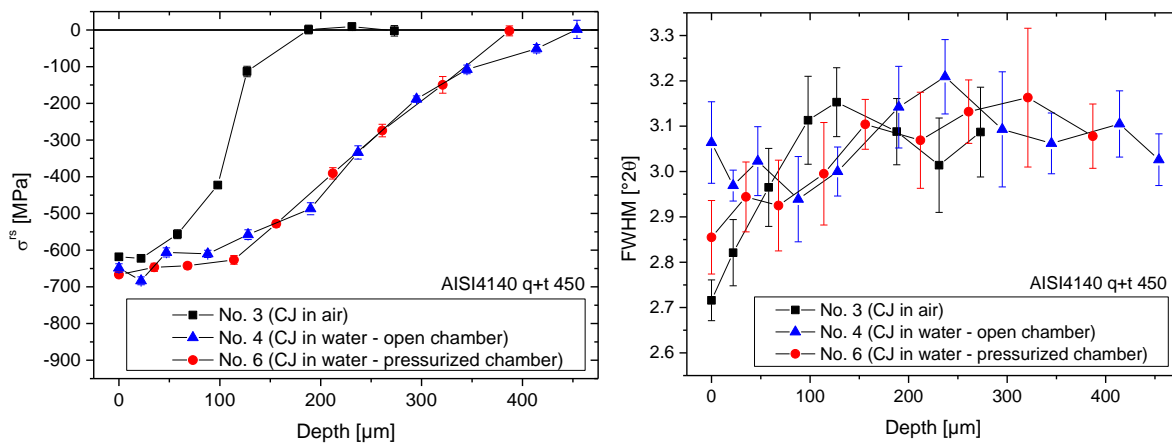


Fig. 2: Residual stress profiles (left) and FWHM distribution (right) after different CP treatments

As can be seen from Fig. 2 (left), maximum residual stresses of approximately -650 MPa were achieved by each CP treatment. Slightly higher residual stress amounts and a pronounced increase of penetration depths could be achieved by using cavitating jets in water, regardless of the applied chamber type. An obvious difference between CP in air and in water also exists with regard to the FWHM values. CP in air shows a remarkable decrease in FWHM values close to the surface, while this decrease is not pronounced for CP in water (open chamber) and little pronounced for CP in water (pressurized chamber).

Fig. 3 shows surface topographies after CP in air (left), CP in open water chamber (middle) and CP in pressurized water chamber (right). The roughness values R_z are 1.02, 1.13 and 1.84, respectively.

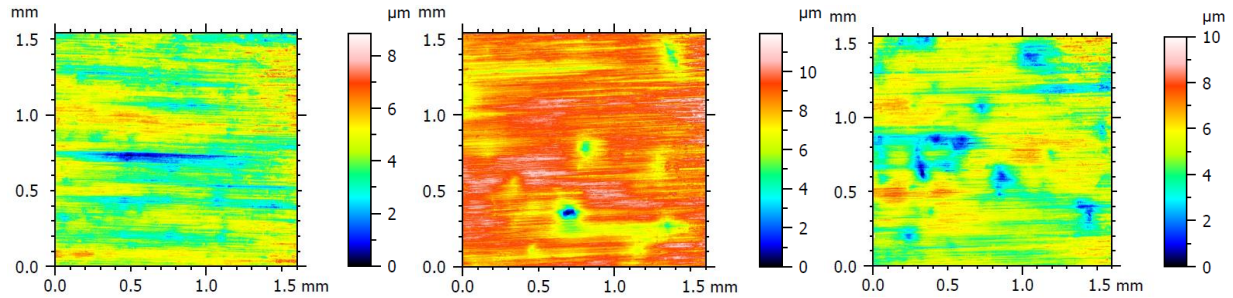


Fig. 3: Surface topographies after CP treatments (left: CP in air; middle: CP in water (open chamber); right: CP in water (pressurized chamber))

As can be seen from Fig. 3, CP in water leads to large and deep cavitation impacts, while the latter are hardly visible after CP in air. While the average projected impact area is around 0.007 mm^2 for CP in air, three to four times larger projected impact surfaces were found after CP in pressurized water chamber. These values are rather difficult to determine because the impact shape changes from smooth and round after CP in air to rather irregular after CP in water, especially when a pressurized chamber is used. This can be explained in terms of the energy introduced into the surface by each impact. Yet, CP in air leads to many small impacts, while the number of impacts after CP in water seems to be limited.

As mentioned previously [6], the introduction of compressive residual stress by cavitating jets in air corresponds to shot peening using small shots at high velocity. Since many impacts apply, the decrease in FWHM is probably due to relieved micro strains, i.e. work-softening. This effect is often perceptible after mechanical surface treatments on AISI4140 in the quenched and tempered state [8, 13, 14]. For instance, [14] found decreasing near-surface FWHM values due to work-softening after machine hammer peening with increasing degrees of local plastic deformation. Oppositely, the introduction of residual stresses by cavitating jets in water corresponds to shot peening using large shots at low velocity [6]. As there is no pronounced difference in impact size after use of open or pressurized chamber, the difference in near-surface FWHM values should be explained in terms of the “cushion” effect of secondary bubbles [7]. Since higher impact energies are generally achieved by using pressurized chambers, an increased proportion of the impact energy seems to be transformed into local plastic deformation work, thus leading to work-softening. Furthermore, the prevailing deformation mechanism according to [15] seems to be plastic stretching, regardless of which type of CP is applied. It is therefore assumed that the “cushion” effect observed in open chambers leads to less pronounced work-hardening or softening, depending on the material used.

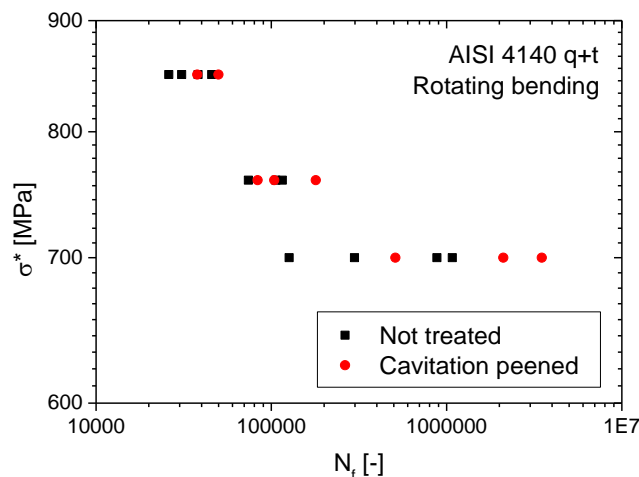


Fig. 4: Fatigue behavior after CP (pressurized chamber), characterized by rotating bending

Fig. 4 shows the S/N curve obtained by rotating bending fatigue tests on cylindrical specimens. Average fatigue lifetimes could obviously be enhanced by means of CP in a pressurized chamber, which is most significant in the HCF range. As aforementioned, hardly any effects of CP on surface roughness and near-surface work-hardening were found. Rather than work-hardening, softening occurred due to dislocation rearrangement. Thus, the effect of CP on fatigue behavior can mainly be attributed to beneficial near-surface compressive residual stresses. Using AISI4140, CP can possibly be used as an effective alternative to conventional shot peening on complex, notched geometries, where the effect of compressive residual stresses on fatigue lifetimes is expected to be more pronounced than on smooth specimens [13]. However, further experiments regarding notch fatigue strength and residual stress stability after CP are necessary for proper assessment.

The question arises how CP generally acts in a benchmark of different mechanical surface treatments on AISI4140. Therefore, residual stress state and FWHM distribution after CP in the pressurized water chamber shall be compared to a variety of mechanical surface treatments on AISI4140. This benchmark was published in [8] and shall now be extended.

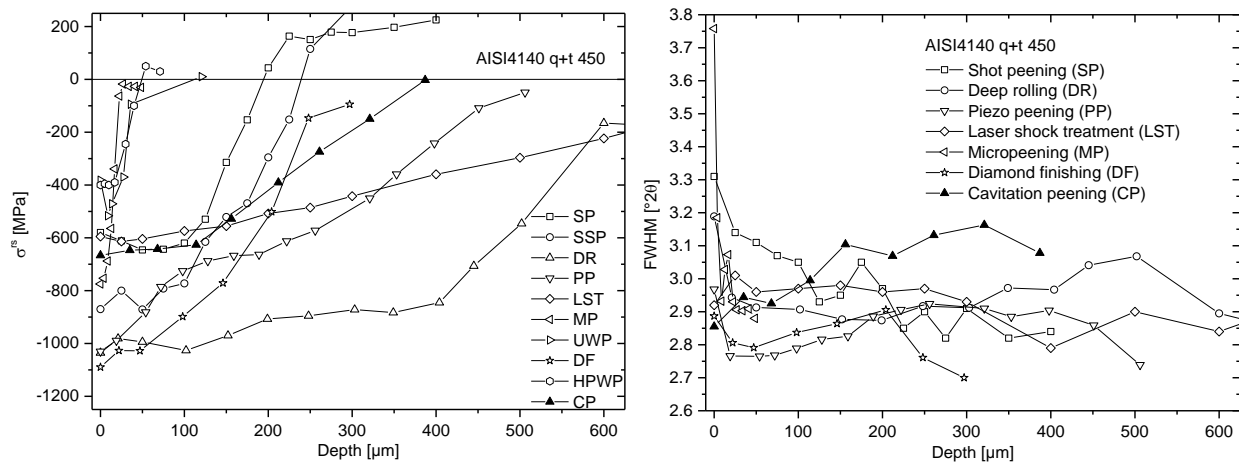


Fig. 5: Residual stress (left) and FWHM profiles (right) after various mechanical surface treatments; diagrams extracted from [8]

Fig. 5 (left) shows residual stresses after various mechanical surface treatments on AISI4140 in a quenched and tempered state (610 °C for high pressure water peening; 450 °C for all other mechanical surface treatments). Selected surface treatments are: Shot peening (“SP”; shot: S170, 56 HRC; pressure: 1.6 bar; Almen intensity: 0.3 mmA) [16], stress peening (“SSP”; shot: S170, 56 HRC; pressure: 1.6 bar; Almen intensity: 0.3 mmA; longitudinal stress state; prestress: 600 MPa) [16], deep rolling (“DR”; pressure: 250 bar; path spacing: 0.04 mm; ball diameter: 6.35 mm), piezo peening (“PP”; frequency: 500 Hz; amplitude: 18 μm ; indenter diameter: 5 mm; path spacing: 0.2 mm) [14], laser shock treatment (“LST”; Nd:glass slab laser; energy density: 168 J/cm²; wavelength: 1053 nm; pulse width: 18 ns; layers: 2; overlap: 50%) [17], micro peening (“MP”; glass beads MS550B; pressure: 1.5 bar; Almen intensity: \sim 0.04 mmN) [18], ultrasonic wet peening (“UWP”; frequency: 20 kHz; process time: 30 min) [19], diamond finishing (“DF”; feed: 0.6 mm; path spacing: 0.04 mm; ball diameter: 2 mm), high pressure water peening (“HPWP”); pressure: 1000 bar; nozzle diameter: 1.5 mm; impact time: 3 s) [20] and cavitation peening in a pressurized water chamber (“CP”; see for parameters above). Fig. 5 (right) shows corresponding FWHM profiles for selected mechanical surface treatments.

Maximum residual stresses similar to shot peening could be achieved by CP together with an increased residual stress penetration depth. Obviously, the assumption concerning the introduction of residual stresses during CP in water chambers, namely, the similarity to shot peening with large shots at low velocity [6], seems to be valid for AISI4140. Indeed, the residual stress profile after CP

in pressurized water chamber is quite similar to the shot peening induced residual stress profile. However, even the chosen shot peening parameter set, which contains a rather low pressure value of 1.6 bar, leads to a contrary effect regarding FWHM values. This is probably due to the high shot peening induced strain rates which lead to very diffuse dislocation arrangements and thus to an increase of FWHM values, which has been discussed in [13].

Conclusions

Residual stress profiles, full width at half maximum distributions and surface roughness values were evaluated after cavitation peening on quenched and tempered low alloy steel AISI4140. The effect of three different types of CP was investigated. Maximum residual stress amounts of approximately -650 MPa in connection with penetration depths of up to 450 μm were found. The different CP treatment types have unique effects on near-surface FWHM values which were explained in terms of micro strains, work-softening and "cushion" effects of secondary cavitation bubbles. Using CP in water (pressurized chamber), the rotating bending fatigue behavior could be enhanced in both HCF and LCF range. In comparison with other mechanical surface treatments, penetration depth of the affected surface layer was intermediate. While maximum residual stress amounts, found at the surface after CP, are comparable to those obtained by shot peening, much higher penetration depths could be achieved.

References

- [1] Soyama, H. et al.: *Journal of Engineering Materials and Technology*, 124 (2002), pp. 135-139.
- [2] Soyama, H. et al.: *JSME International Journal*, 38B (1995), pp. 245-251.
- [3] Soyama, H.: *Journal of Engineering Materials and Technology*, 126 (2004), pp. 123-128.
- [4] Soyama, H. et al.: *Surface and Coatings Technology*, (2011), pp. 3167-3174.
- [5] Soyama, H. and Yamada, N.: *Materials Letters*, 62 (2008), pp. 3564-3566.
- [6] Soyama, H., et al.: in *Proc. 9th Pacific Rim Int. Conf. on Water Jetting Technology*, (2009), pp. 133-137.
- [7] Soyama, H.: *Wear*, 297 (2013), pp. 895-902.
- [8] Klumpp, A. et al.: in *Proc. ICSP12* (2014), pp. 12-24.
- [9] Soyama, H.: *Journal of Fluid Science and Technology*, 9, (2014), paper No. 13-00238, pp. 1-12.
- [10] Soyama, H.: *Journal of Fluids Engineering*, 133, (2011), paper No. 101301, pp. 1-11.
- [11] Soyama, H. and Mikami, M.: *Proc. Annual Meeting for Water Jet Technology*, (2015), pp. 49-52.
- [12] Macherauch, E. and Müller, P.: *Z. angew. Physik*, 13.7 (1961), pp. 305-312.
- [13] Schulze, V.: *Modern mechanical surface treatments: states, stability, effects*. John Wiley & Sons, 2006.
- [14] Lienert, F. et al.: *Materials Science Forum*, 768 (2014), pp. 526-533.
- [15] Wohlfahrt, H.: *Eigenspannungen Entstehung-Messung-Bewertung*. Oberursel (1983), pp. 301-319.
- [16] Wick, A.: *PhD Thesis*, Universität Karlsruhe (TH), 1999.
- [17] Menig, R. et al.: in *Proc. ICSP8* (2003), pp. 498-504.
- [18] Weingärtner, R. et al.: in *Proc. ICSP12* (2014), pp. 31-36.
- [19] Weingärtner, R. et al.: *Materials Science Forum*, 768 (2014), pp. 580-586.
- [20] Kroos, F.: *PhD Thesis*, Universität Hannover, 1995.